Division Pharmaceutics[1], Department of Pharmacy, School of Pharmacy, University of Oslo; PCI Biotech AS[2], Oslo, Norway; Department of Physics and Mathematics[3], University of Insubria at Como, Italy

Physicochemical characterization of the photosensitizers $TPCS_{2a}$ and $TPPS_{2a}$ 1. Spectroscopic evaluation of drug – solvent interactions

M. Lilletvedt[1], H. H. Tønnesen[1], A. Høgset[2], L. Nardo[3], S. Kristensen[1]

Received January 26, 2010, accepted February 8, 2010

Marianne Lilletvedt, School of Pharmacy, Department of Pharmacy, University of Oslo, P. O. box 1068 Blindern, N-0316 Oslo, Norway
marianne.lilletvedt@farmasi.uio.no

Pharmazie 65: 588–595 (2010) *doi: 10.1691/ph.2010.0025*

The spectroscopic properties of the patented photosensitizer meso-tetraphenyl chlorin disulphonate ($TPCS_{2a}$), intended for use in photochemical internalization (PCI) technology, and the chemically related photosensitizer meso-tetraphenyl porphyrin disulphonate ($TPPS_{2a}$) were characterized in 14 organic solvents of varying polarity and amphiprotic properties. Absorption spectra and fluorescence emission spectra were acquired, and Stokes' shifts and fluorescence quantum yields determined. These investigations yield information on the physicochemical interactions between the photosensitizers and their surroundings (i.e., the physiological environment *in vivo* or the vehicle *in vitro*), which is essential for the further development of drug formulations. $TPPS_{2a}$ and $TPCS_{2a}$ are rigid molecules, built up by conjugated ring systems which possess limited interactions with the surroundings in the ground state (S_0). Accordingly, only small spectral shifts were observed in the absorption spectra, as well as in the fluorescence emission spectra. $TPPS_{2a}$ is spatially more planar than $TPCS_{2a}$, which is twisted as a result of reduction of a double bond in the core. However, the two compounds were quite similarly influenced by properties of the solvents, indicating that twisting has limited importance in the interactions of the two photosensitizers with their environment. Both compounds possess a high character of π-π^* transition upon light exposure, supported by high molar absorption coefficients. The fluorescence quantum yields (Φ_f) were influenced by solvent properties to a larger extent than the spectral shifts. This might indicate that the reactivity of the first excited singlet state (S_1^*) significantly depends on the properties of the surroundings.

1. Introduction

The novel photosensitizer meso-tetraphenyl chlorin disulphonate ($TPCS_{2a}$) is to be used in the patented technology photochemical internalization (PCI). The PCI technology has recently been reviewed (Norum et al. 2009; Berg et al. 2006; Høgset et al. 2004). The photosensitizer meso-tetraphenyl porphyrin disulphonate ($TPPS_{2a}$) is the starting material for the synthesis of $TPCS_{2a}$ and also an important degradation product of the latter. It will be used as reference substance in this work. PCI is applied for light-directed drug delivery of chemotherapeutics and macromolecules to the cytosol (Berg et al. 1999). In PCI technology for anticancer treatment, the photosensitizer and an anticancer drug are administered, usually separately. When the photosensitizer and the drug are endocytosed by a target cell, the photosensitizer remains in the membrane of the endocytic vesicles, endosomes and lysosomes, due to its amphiphilic nature, while the drug is trapped inside the vesicles. The photosensitizer will absorb visible light during tumor illumination, which leads to the creation of reactive oxygen species (ROS) like singlet oxygen ($^1O_2$) and, consequently, rupture of endocytic vesicles. The intact drug is then released to the cytosol and can reach the intracellular target (Prasmickaite et al. 2001).

$TPPS_{2a}$ and $TPCS_{2a}$ are synthetic compounds of the porphyrin and chlorin types, respectively. Their structural formulas are shown in Fig. 1. Both porphyrins and chlorins occur in nature, e.g., as heme in the erythrocytes significant for delivery of oxygen *in vivo* (Buchler 1978; James 1978), and chlorophyll in green leaves vital for photosynthesis (Bonnett 1978).

The absorption spectra of both porphyrins and chlorins are characterized by a very intense band, named the Soret band, around 400 nm, and by four additional minor absorption bands in the visible region (Q bands), shifted to the red with respect to the Soret band (Buchler 1978). The spectra reflect the remarkable complexity of the chromophores. The chlorins have a characteristic red band in their absorption spectra (Gouterman 1961), which is notably more intense than the corresponding band of porphyrins and can be utilized clinically in photodynamic therapy (PDT). It is well-known that porphyrins and chlorins have a small energy gap between the lowest singlet and triplet states, and that intersystem crossing (ISC) to the triplet state can be very

Abbreviations: ACN = acetonitrile; API = active pharmaceutical ingredient; AUC = area under the curve; DMF = dimethyl formamide; DMSO, dimethyl sulfoxide; € = molar absorption coefficient; EtOH = ethanol; ISC = intersystem crossing; MeOH = methanol; $^1O_2$ = singlet oxygen; PCI = photochemical internalization; PDT = photodynamic therapy; RSD = relative standard deviation; ROS = reactive oxygen species; S_0 = ground state; S_1^* = first excited singlet state; THF = tetrahydrofuran; $TPCS_{2a}$ = meso-tetraphenyl chlorin disulphonate; $TPPS_{2a}$ = meso-tetraphenyl porphyrin disulphonate; Φ_f = fluorescence quantum yield.

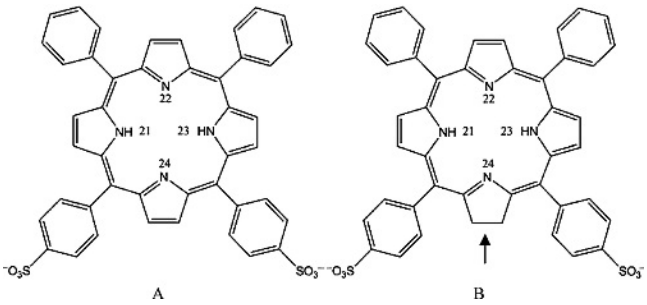

Fig. 1: Structural formulas of $TPPS_{2a}$ (A) and $TPCS_{2a}$ (B). The difference between the two compounds are structurally only a double bond in one pyrrole ring (indicated by an arrow). The numbering of atom positions are in accordance with the provided numbering scheme (Bonnett R (1978) Nomenclature. In: Dolphin D (ed.) The Porphyrins, New York, Vol. I Structure and Synthesis Part A, p. 9)

efficient (Suslick and Watson 1992). This leads to high production of ROS, and makes porphyrin-related compounds preferred for PDT and PCI anticancer treatment.

The aim of this work was to characterize possible intra- and intermolecular interactions of $TPCS_{2a}$ and $TPPS_{2a}$ in solution. Absorption and fluorescence emission spectra and fluorescence quantum yields of the two compounds were recorded in a range of solvents of varying polarity and amphiprotic properties. Characterization of physicochemical properties, e.g., drug-vehicle interactions, is of pharmaceutical importance and thus valuable in the further drug formulation process.

2. Investigations, results and discussion

2.1. Molecular properties

The two photosensitizers included in this study are structurally very similar, as shown in Fig. 1. The only difference is a double bond in the core of $TPPS_{2a}$, which is reduced in $TPCS_{2a}$. This is a general distinction between porphyrins and chlorins. As a result, $TPCS_{2a}$ can appear as three different stereoisomers. 3D models of $TPPS_{2a}$ and one of the isomers of $TPCS_{2a}$ are presented in Fig. 2, which emphasizes the spatial influence of the double bond. $TPPS_{2a}$ is planar, while all three isomers of $TPCS_{2a}$ are twisted around the core. The two molecules are rigid, built up by electronically conjugated ring systems. The flat molecule $TPPS_{2a}$ contains electrons of high mobility, while the electrons might possess somewhat reduced mobility in the twisted $TPCS_{2a}$.

Two sulphonate groups are present in both molecules (Fig. 1). Sulphonate groups are known for their electron-withdrawing force (Burgoyne 1979, Seliskar and Brand 1971), and will to some extent draw the electrons out of the core of both the molecules. According to Ghosh (1996), enhanced electronic effects are introduced when the electron-withdrawing groups are present in para positions in tetraphenyl porphyrins, as is the case here. The electron distribution will to some extent be influenced by the distortion of planarity in $TPCS_{2a}$ (Fig. 2). Both porphyrin and chlorin molecules have extensive electron delocalization in the nucleus (Pasternack et al. 1972). Conjugation is known to be further extended in porphyrins compared to chlorins, where one of the rings is reduced (Gouterman et al. 1963). The electronic states of the porphyrin monomer are described by Gouterman's four orbital model (π-π^* orbitals; Suslick and Watson 1992).

Two of four nitrogen atoms are protonated in the molecular cores, when the molecules exist as free base. Thus, the cores will not be charged (Pasternack et al. 1972). However, as the two sulphonate substituents have pK_a values ≤ 1 (Pasternack et al. 1972), the free base forms of $TPPS_{2a}$ and $TPCS_{2a}$ will be dianionic.

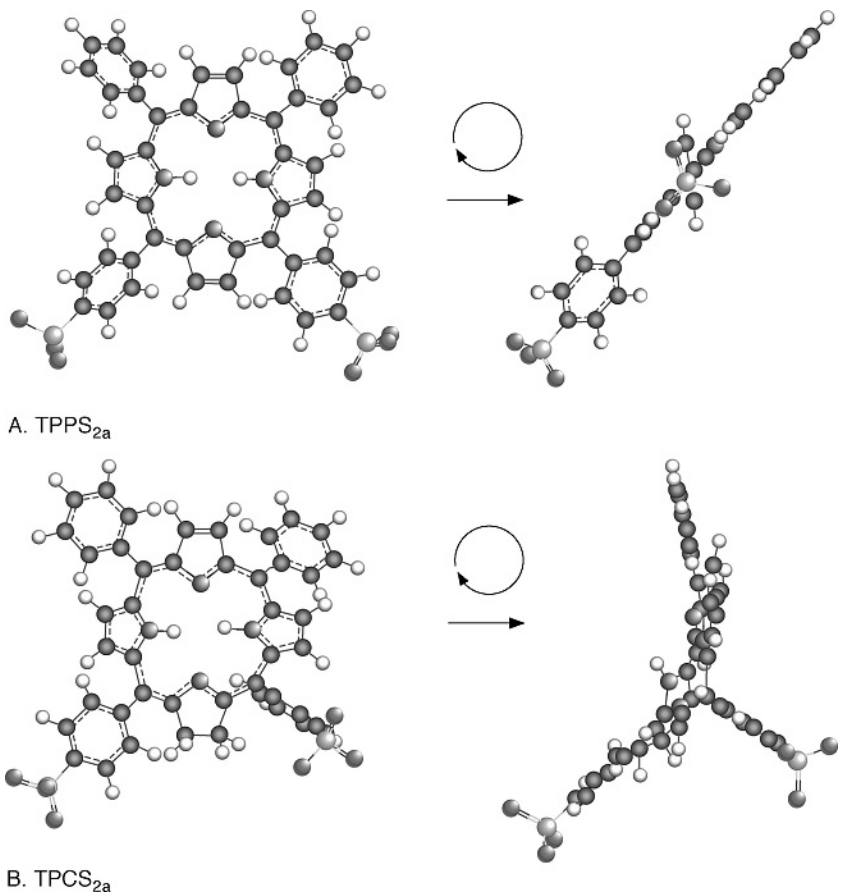

Fig. 2: Spatial models of $TPPS_{2a}$ and $TPCS_{2a}$. 3D visualization of the molecules illustrate the difference in planarity between the compounds when rotating the molecules. $TPPS_{2a}$ (A) is more planar than $TPCS_{2a}$ (B). The computer program ChemBioDraw Ultra 11.0 were used in the process of making the illustrations

Table 1: Calculated distance* (Å) between N-atoms in $TPPS_{2a}$ and $TPCS_{2a}$**

N-atom	$TPPS_{2a}$	$TPCS_{2a}$
N(22) and N(24)	4.2 Å	4.3 Å
N(21) and N(23)	4.2 Å	4.3 Å
N(21) and N(24)	3.0 Å	3.1 Å
N(21) and N(22)	3.0 Å	3.0 Å
N(23) and N(24)	3.0 Å	3.1 Å
N(22) and N(23)	3.0 Å	3.0 Å

*The calculations were performed by means of ChemBioDraw Ultra 11.0
*Numbering is illustrated in Fig. 1

The core cavities of $TPPS_{2a}$ and $TPCS_{2a}$ may interact with small solvent molecules, or include metal ions when present. The size of the cavity is not highly altered by reduction of the one π-bond, even though $TPCS_{2a}$ is twisted around the core (Fig. 2). Calculations of the spacing between the nitrogen moieties in the core of $TPPS_{2a}$ and $TPCS_{2a}$ were performed *in silico* using the known atom coordinates of the nitrogen atoms. The distance between the atoms 1 and 2 is given by Eq. (1):

$$\text{Distance} = \sqrt{((x2 - x1)^2 + (y2 - y1)^2 + (z2 - z1)^2)} \quad (1)$$

where x1, y1 and z1 are the spatial coordinates of atom 1, and x2, y2 and z2 are the spatial coordinates of atom 2 (ChemBioDraw Ultra 11.0). The distance between the nitrogen moieties of the molecular centre is slightly increased for all isomers of $TPCS_{2a}$ compared to $TPPS_{2a}$. However, the spaces between the twisted N(24) and N(21); N(22); and N(23), respectively, and N(21) – N(23) are only 2–3 % larger in $TPCS_{2a}$ than in $TPPS_{2a}$ (Table 1). These calculations refer to the illustrated isomer of $TPCS_{2a}$ in Fig. 1, but the distances are not highly altered in any of the isomers. Although such a small difference in the cavity size can be disregarded in the elucidation of the intramolecular charge distribution and the assessment of the interactions of the two compounds with solvent molecules in solution, it may possibly be sufficient to influence the metal ion chelating properties of the compounds. This subject is beyond the scope of the present article, but will be investigated in the future.

The salts of $TPPS_{2a}$ and $TPCS_{2a}$ possess different counterions, respectively triethylammonium and monoethanolammonium, which were made available by PCI Biotech AS and compared in this study. Dissimilar counterions may theoretically influence the properties of $TPPS_{2a}$ and $TPCS_{2a}$ in solution. However, as the concentrations of $TPPS_{2a}$ and $TPCS_{2a}$ were kept very low throughout this study ($<10^{-7}$ M), the amount of counterions was considered insignificant to influence the measurements. Porphyrin-related compounds are known for the formation of aggregates (stacking), leading e.g., to quenching of fluorescence (Cunderlikova et al. 2001; Dairou et al. 2002). Aggregation can be avoided by working at low concentrations (< 1 – 50 μM; Maiti et al. 1998; Winters et al. 2007). In our study, stacking is unlikely to occur at the low concentrations of $TPPS_{2a}$ and $TPCS_{2a}$ used.

2.2. Absorption properties and solvent interactions

The absorption spectra of $TPPS_{2a}$ and $TPCS_{2a}$ are only slightly dependent on the solvent properties in organic media (Table 2 and 3). This indicates that only minor interactions take place between these molecules in the ground state (S_0) and the surrounding solvent molecules. Minor solvent effects have also been reported for planar porphyrins in previous literature (Takeda and Sato 1995). Moreover, the absorption properties of $TPPS_{2a}$ and $TPCS_{2a}$ appear to be quite similar in organic solvents.

As an example, the UV-visible absorption spectrum of $TPPS_{2a}$ obtained for the compound dissolved in methanol, is shown in Fig. 3A. The Soret band of $TPPS_{2a}$ (peak 2 in Fig. 3A) is located at 413–419 nm in organic media (Table 2). This band is the most intense in the UV-visible absorption spectrum. In addition, the Soret band has a broad shoulder (labelled 1 in Fig. 3A) and a tail in the UV-region. The shape of the Soret band is structureless, which is consistent with the planarity of $TPPS_{2a}$ (Fig. 2) and with the consequent ability of a free intramolecular flow of π and n-electrons, as mentioned in Sec. 2.1. The UV-visible absorption spectrum of $TPCS_{2a}$ in methanol is reported in Fig. 3B. Similarly to $TPPS_{2a}$, the absorption spectrum of $TPCS_{2a}$ is only slightly affected by the properties of the organic medium in which the compound is dissolved. In addition, the Soret band is the most intense in the UV-visible range. However, the Soret band of $TPCS_{2a}$ is split into three distinct peaks (labelled 1, 2a and 2b in Fig. 3B), located at respectively 367–373, 404–408 and 416–421 nm in the organic solvents (Table 3). The only exceptions to this rule are observed in ethylene glycol, DMSO and DMF, where peak 2a is almost absent (data not shown). Conversely, when dissolved in chloroform, $TPPS_{2a}$ gives an unusually wide Soret band with an indication of a peak at ~405 nm, similar to that revealed for $TPCS_{2a}$ in the majority of the solvents and indicated as peak 2a (Fig. 3B). The splitting of the Soret band of $TPCS_{2a}$ is likely caused by the reduced mobility of the core electrons due to molecular twisting. The shoulder and the tail of the Soret band of $TPPS_{2a}$ (labeled as 1 in Fig. 3A) presumably correspond to the more prominent peak at 367–373 nm of $TPCS_{2a}$ (correspondingly labelled 1 in Fig. 3B). The wavelength distance between the peaks 2a and 2b of $TPCS_{2a}$ remains almost constant (~12 nm) in the organic media. The

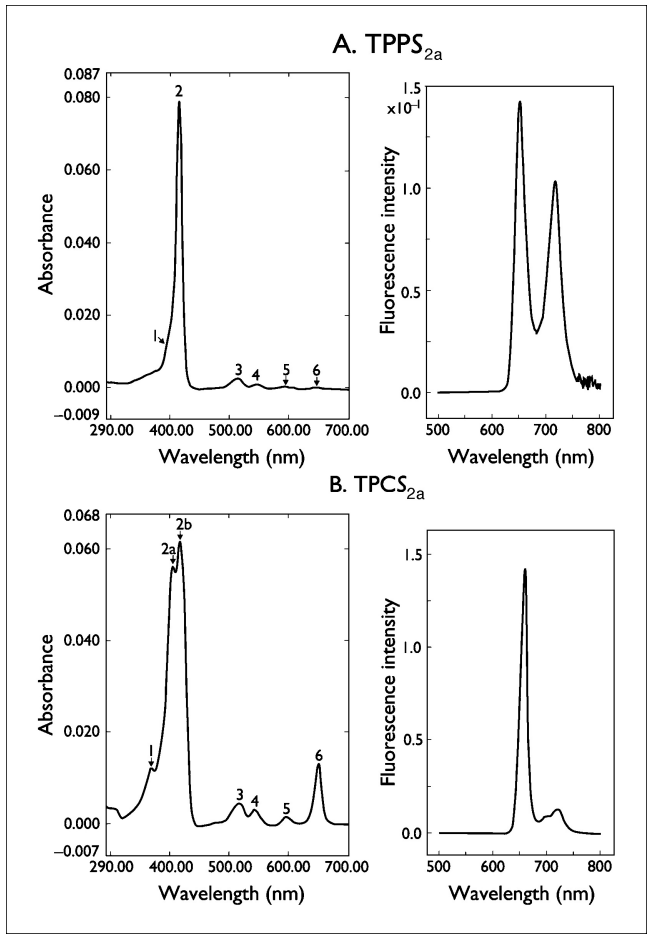

Fig. 3: Absorption and fluorescence emission spectra of $TPPS_{2a}$ (A) and $TPCS_{2a}$ (B) in methanol

Table 2: Absorption and fluorescence properties of $TPPS_{2a}$ in pure solvents

Solvent	λ_{abs} (nm)	v (cm^{-1}) (10^4)	λ_{em} (nm)	v (cm^{-1}) (10^4)	Stokes' shift (cm^{-1})	Φ_f
Ethylene glycol	417	2.40	649, 715	1.54, 1.40	8 600, 10 000	0.129 ± 0.026
Methanol	413	2.42	650, 715	1.54, 1.40	8 800, 10 200	0.038 ± 0.011
Ethanol	413	2.42	650, 715	1.54, 1.40	8 800, 10 200	0.041 ± 0.033
2-Propanol	415	2.41	650, 717	1.54, 1.40	8 700, 10 100	0.062 ± 0.015
1-Butanol	416	2.40	651, 718	1.54, 1.39	8 700, 10 100	0.073 ± 0.005
Dimethyl sulfoxide	419	2.39	651, 718	1.54, 1.39	8 500, 9 900	0.110 ± 0.005
Dimethyl formamide	418	2.39	651, 718	1.54, 1.39	8 600, 10 000	0.109 ± 0.009
Acetonitrile	415	2.41	650, 717	1.54, 1.39	8 700, 10 100	0.076 ± 0.009
Acetone	415	2.41	650, 717	1.54, 1.39	8 700, 10 100	0.034 ± 0.006
Tetrahydrofuran	417	2.40	651, 718	1.54, 1.39	8 600, 10 100	0.062 ± 0.006
Chloroform	419	2.39	655, 720	1.53, 1.39	8 600, 10 000	0.009 ± 0.006
Ethyl acetate	415	2.41	650, 717	1.54, 1.39	8 700, 10 100	0.080 ± 0.026
Diethyl ether	(N.S.D)*	-	-	-	-	-
Cyclohexane	(N.S.D)*	-	-	-	-	-

*N.S.D = not spectrophotometrically detectable
λ = wavelength
v = wavenumber Stokes' shift (cm^{-1}) = $(1/\lambda_{abs}(nm))-(1/\lambda_{em}(nm)) \times 10^7$
Φ_f (fluorescence quantum yield) = $(AUC_{sample}/AUC_{quinine\ sulphate\ reference}) \times (Abs_{quinine\ sulphate\ reference}/Abs_{sample}) \times 0{,}51 \times (n_{solvent}^2/n_{water}^2)$, where n = refractive index

absorption maximum 2b is more intense than 2a in all solvents, and is therefore considered as the main peak in the further evaluations.

The absorption spectra of both $TPPS_{2a}$ and $TPCS_{2a}$ additionally contain four minor peaks (Q bands) in the range 500–700 nm (labelled 3, 4, 5 and 6 in Fig. 3), which are most prominent for $TPCS_{2a}$. In particular, a distinct absorption maximum (labelled 6 in Fig. 3B) is observed at 650–652 nm for $TPCS_{2a}$ dissolved in the organic media, which is characteristic for chlorines. The PCI technology takes advantage of the presence of this red absorption band, as red light penetrates deeper into tissues than light of shorter wavelengths (Dawson et al. 1980).

Porphyrin-like compounds in general possess high molar absorption coefficients, which is advantageous when using these substances as photosensitizers. The molar absorption coefficient of $TPPS_{2a}$ in methanol at the Soret band peak was determined to $\varepsilon_{413} = 503\,000\ M^{-1}cm^{-1}$ (RSD = 2.8%; n = 18), indicating an efficient transition of π-π* character upon light absorption, as expected (Gouterman 1961; Reddi and Jori 1988; Valeur 2002). In comparison, the molar absorption coefficients of the three peaks that appeared within the Soret band of $TPCS_{2a}$ dissolved in methanol are $\varepsilon_{369} = 47\,000\ M^{-1}cm^{-1}$ (RSD = 5.5 %; n = 24), $\varepsilon_{404} = 184\,000\ M^{-1}cm^{-1}$ (RSD = 3.7 %; n = 24) and $\varepsilon_{416} = 201\,000\ M^{-1}cm^{-1}$ (RSD = 3.3 %; n = 24), which are also consistent with π-π* transitions. These molar absorption coefficients sum up to $432\,000\ M^{-1}cm^{-1}$, which is in the same range as the molar absorption coefficient of $TPPS_{2a}$. Therefore, we conclude that the origin of the Soret bands of $TPPS_{2a}$ and $TPCS_{2a}$ are very similar. In particular, the splitting of the Soret band in three peaks for $TPCS_{2a}$ is unlikely to be caused by the coexistence of the three different stereoisomers of $TPCS_{2a}$. The values of the molar absorption coefficients for both compounds are nearly constant independent of drug concentration ($10^{-6}-10^{-7}$ M; RSD $\leq$ 5.5 %, n = 18–24), and the spectral shapes do not change. This supports the assumption that aggregation does not take place under the given experimental conditions (Akins et al. 1996; Gerhardt et al. 2003; Maiti et al. 1998; Smith 1985).

The molar absorption coefficient of the Q band of $TPCS_{2a}$ at 651 nm in methanol was determined to $\varepsilon_{651} = 41\,000\ M^{-1}cm^{-1}$ (RSD = 4.6 %; n = 24). Absorption bands present in the red part

Table 3: Absorption and fluorescence properties of $TPCS_{2a}$ in pure solvents

Solvent	λ_{abs} (nm)	v (cm^{-1}) (10^4)	λ_{em} (nm)	v (cm^{-1}) (10^4)	Stokes' shift (cm^{-1})	Φ_f
Ethylene glycol	419	2.39	655	1.53	8 600	0.300 ± 0.011
Methanol	416	2.40	654	1.53	8 700	0.200 ± 0.036
Ethanol	417	2.40	654	1.53	8 700	0.245 ± 0.036
2-Propanol	417	2.40	654	1.53	8 700	0.249 ± 0.041
1-Butanol	418	2.39	655	1.53	8 700	0.262 ± 0.021
Dimethyl sulfoxide	421	2.38	656	1.52	8 500	0.328 ± 0.022
Dimethyl formamide	420	2.38	655	1.53	8 500	0.243 ± 0.047
Acetonitrile	417	2.40	655	1.53	8 700	0.216 ± 0.011
Acetone	417	2.40	654	1.53	8 700	0.196 ± 0.003
Tetrahydrofuran	419	2.39	655	1.53	8 600	0.254 ± 0.014
Chloroform	(N.S.D)*	-	-	-	-	-
Ethyl acetate	(N.S.D)*	-	-	-	-	-
Diethyl ether	(N.S.D)*	-	-	-	-	-
Cyclohexane	(N.S.D)*	-	-	-	-	-

*N.S.D. = not spectrophotometrically detectable
λ = wavelength
v = wavenumber
Stokes' shift (cm^{-1}) = $(1/\lambda_{abs}(nm))-(1/\lambda_{em}(nm)) \times 10^7$
Φ_f (fluorescence quantum yield) = $(AUC_{sample}/AUC_{quinine\ sulphate\ reference}) \times (Abs_{quinine\ sulphate\ reference}/Abs_{sample}) \times 0{,}51 \times (n_{solvent}^2/n_{water}^2)$, where n = refractive index

Table 4: Solvent properties

Category	Solvent	π*	α	β	ε	n	$(\varepsilon-1)/(2\varepsilon+1)$	$(n^2-1)/(2n^2+1)$	Δf
Polar	Ethylene glycol	0.92	0.90	0.52	37.70	1.431	0.480	0.206	0.275
Protic	Methanol	0.60	0.93	0.62	32.66	1.328	0.477	0.169	0.309
	Ethanol	0.54	0.83	0.77	24.55	1.361	0.470	0.181	0.289
	2-Propanol	0.48	0.76	0.95	19.92	1.377	0.463	0.187	0.276
	1-Butanol	0.47	0.79	0.88	17.51	1.399	0.458	0.195	0.264
Polar	Dimethyl sulfoxide	1.00	0.00	0.76	48.90	1.478	0.485	0.221	0.264
Non-protic	Dimethyl formamide	0.88	0.00	0.69	37.60	1.430	0.480	0.205	0.275
	Acetonitrile	0.75	0.19	0.31	35.94	1.344	0.479	0.175	0.305
	Acetone	0.71	0.08	0.48	20.60	1.359	0.464	0.180	0.284
	Tetrahydrofuran	0.58	0.00	0.55	7.58	1.407	0.407	0.198	0.210
	Chloroform	0.58	0.44	0.00	4.81	1.446	0.359	0.211	0.148
	Ethyl acetate	0.45	0.00	0.55	6.02	1.372	0.385	0.185	0.200
	Diethyl ether	0.27	0.00	0.47	4.34	1.353	0.345	0.178	0.167
Non-polar	Cyclohexane	0.00	0.00	0.00	2.02	1.426	0.202	0.204	-0.002

Solvent polarity (π* parameter), proton donor property (α parameter) and proton acceptor property (β parameter) are taken from Appendix 4 in Suppan and Ghoneim (1997).
ε = dielectric constant. n = refractive index. Solvent orientation polarizability, $\Delta f = (\varepsilon-1)/(2\varepsilon+1) - (n^2-1)/(2n^2+1)$ (Lakowicz 1999)

of the spectrum represent the electronic transitions of lowest energy, and are generally considered to be of n-π* character in nitrogen heterocyclics (Calvert and Pitts 1966). However, the high molar absorption coefficient indicates a high degree of π-π* electronic transition.

The properties of the solvents used in the present work are given in Table 4. Perturbations of the electronic energy levels of a molecule in solution may occur by the so called general solvent effects, as a result of the refractive index (n) and dielectric constant (ε) of the solvent. Such perturbations may be revealed by observing spectral shifts of the solute with changes in the polarity and polarizability of the solvent. The absorption spectral shifts of $TPPS_{2a}$ and $TPCS_{2a}$ were observed by evaluation of the Soret band of each compound. The main peak at 416–421 nm (2b in Fig. 3B) was selected in case of $TPCS_{2a}$. The spectral shifts are very small. This further emphasizes that $TPPS_{2a}$ and $TPCS_{2a}$ are rigid molecules in the S_0 state that are not easily influenced by the surroundings. Nevertheless, a slight bathochromic (red) shift of the absorption maximum is observed for both compounds when increasing the solvent transient electronic polarizability, measured as the refractive index term of the solvent orientation polarizability, Eq. (2) (Lakowicz 1999; LeRosen and Reid 1952):

$$\text{Refractive index term} = \frac{n^2-1}{2n^2+1} \qquad (2)$$

where n is the solvent refractive index, given in Table 4. The functional dependence of the absorption maximum wavelength from the refractive index term is approximately linear ($TPPS_{2a}$: $R^2 = 0.873$; $TPCS_{2a}$: $R^2 = 0.932$, Fig. 4A and 4B, respectively). The bathochromic shift is larger for $TPPS_{2a}$ than for $TPCS_{2a}$, as demonstrated by the steeper slope of the regression line (+27%, Fig. 4).

Increased solvent polarity, measured as the π* parameter (Kamlet et al. 1983), also leads to slight bathochromic shifts, that are nearly linear in the highly polar solvents i.e., ($\pi^* \geq 0.6$; n = 6; $TPPS_{2a}$: $R^2 = 0.942$; $TPCS_{2a}$: $R^2 = 0.915$; data not shown). However, the experimental error (± 1 nm) and very small shift range (4–6 nm) should be kept in mind. Minimal solvatochromic shifts in polar solvents is characteristic for non-polar solutes (Suppan and Ghoneim 1997), and indicates delocalization of charge into the extended conjugated ring system. The red shifts as a function of increased polarity, which are typical for π-π* transitions (Calvert and Pitts 1966), are slightly larger for $TPPS_{2a}$ compared to $TPCS_{2a}$, as demonstrated by a 15 % steeper slope in the highly polar solvents.

The influence of specific solvent interactions on the absorption properties of $TPPS_{2a}$ and $TPCS_{2a}$ was evaluated by the effect of amphiprotic solvents on the Soret bands. Plots of absorption maximum (nm) versus solvent proton donor properties, measured as the α-parameter, or solvent proton acceptor properties, measured as the β-parameter (Kamlet et al. 1983), show similar patterns for $TPPS_{2a}$ and $TPCS_{2a}$ in all the solvents, but the plots are hard to interpret (data not shown). In conclusion, $TPPS_{2a}$ and $TPCS_{2a}$ behave very similarly and are hardly influenced by the surrounding media.

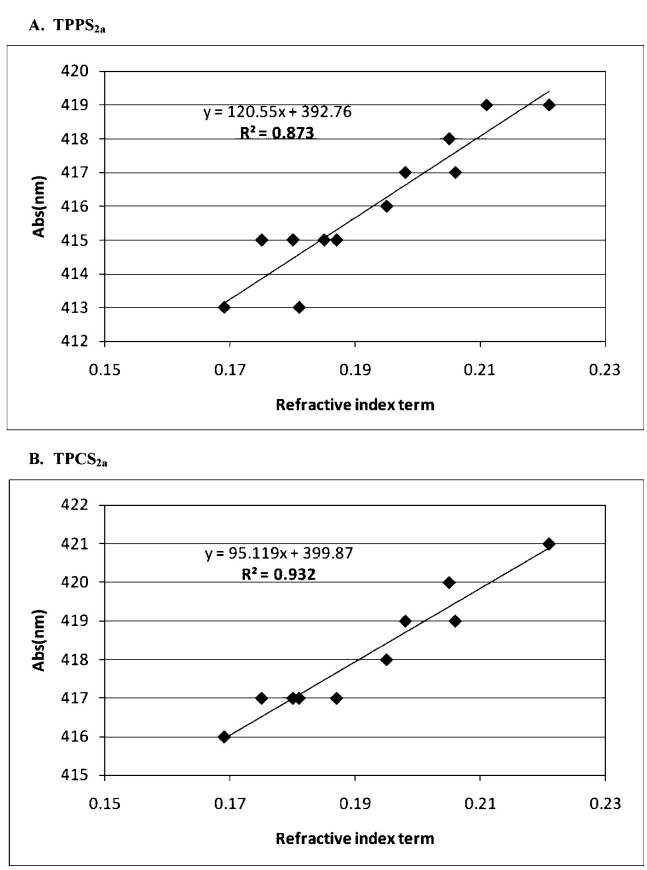

Fig. 4: Plots of absorption maximum (nm) of $TPPS_{2a}$ (A) and $TPCS_{2a}$ (B) as a function of solvent refractive index term

2.3. Fluorescence emission spectra and solvent interactions

Fluorescence emission spectra upon excitation of $TPPS_{2a}$ and $TPCS_{2a}$ at the absorption peak of the Soret band (i.e., peak 2 for $TPPS_{2a}$ and peak 2b for $TPCS_{2a}$ in Fig. 3) were recorded in various organic solvents (Table 2 and 3). $TPPS_{2a}$ emits fluorescence in two distinct bands with maxima at 649–655 nm and 715–720 nm, respectively, in all media in which the molecule can be spectrophotometrically detected (Table 2), as illustrated by the fluorescence emission spectrum in methanol (Fig. 3A). In chloroform, the red-shifted emission peak is split into two distinct maxima at 715 and 721 nm, respectively. $TPCS_{2a}$ displays a corresponding emission band at maximum 654–655 nm in the organic solvents (Table 3). Two minor peaks at ~700 nm and 720 nm correspond to the single red-shifted peak of $TPPS_{2a}$. The peak appearing at ~700 nm for $TPCS_{2a}$ in all solvents seems to be included in the dominating peak at 715–720 nm in the fluorescence emission spectra of $TPPS_{2a}$, except in chloroform. The peak at ~650 nm is more intense compared to the red-shifted peaks for both compounds; by a factor about 1.5 for $TPPS_{2a}$ ($n = 12$ solvents) and about 10 for $TPCS_{2a}$ ($n = 10$ solvents). Thus, fluorescence emission peaks at very similar wavelengths are observed for the two compounds, but the intensity ratio between them is different.

A fluorescence emission spectrum generally appears to be a mirror image of the absorption spectrum. Deviations usually indicate a different geometric arrangement of nuclei in the excited state compared to the ground state (Lakowicz 1999). As the raw material of $TPPS_{2a}$ contains only one isomeric compound, the emission bands are likely to represent various transients of $TPPS_{2a}$ in the lower excited singlet state (S_1*). The Stokes' shifts of the two peaks (8 500 – 8 800 cm^{-1} and 9 900 – 10 200 cm^{-1}, Table 2) indicate S_1* states at different energetic levels caused by several sterical conformations of $TPPS_{2a}$ in the excited state. The same phenomenon seems to be observed for $TPCS_{2a}$, since the fluorescence spectra of $TPPS_{2a}$ and $TPCS_{2a}$ are quite similar, as described above.

The fluorescence emission spectra of both $TPPS_{2a}$ and $TPCS_{2a}$ are only slightly sensitive to the polarity and H-bonding properties of their environment (Table 2 and 3). The loss of energy between absorption and emission of light, i.e., Stokes' shift, is generally a result of several dynamic processes. In non-polar solvents, Stokes' shifts would essentially represent energy losses due to dissipation of vibrational energy, but they could not be evaluated due to insolubility of both $TPPS_{2a}$ and $TPCS_{2a}$ in such media. Stokes' shifts in polar solvents additionally result from both reorientation of solvent molecules around the excited state molecular dipole moment (μ*) of the solute molecule (in the case where it is significantly different from that of the ground state molecule) and specific interactions with the solvent (e.g., hydrogen bonding or formation of charge transfer complexes) (Lakowicz 1999). For both $TPPS_{2a}$ and $TPCS_{2a}$, only tiny variations in the Stokes' shifts (maximum difference = 300 cm^{-1}) were observed when changing the solvent.

General solvent interactions with the solutes in the S_1* state are in general due to solvent orientation polarizability, Δf, which is given by Eq. (3):

$$\Delta f = (\varepsilon - 1)/(2\varepsilon + 1) - (n^2 - 1)/(2n^2 + 1) \qquad (3)$$

where ε is the dielectric constant and n is the refractive index, given in Table 4 (Lakowicz 1999). The small changes in the Stokes' shifts indicate limited influence of Δf, suggesting that the change in dipole moment upon excitation ($\mu \rightarrow \mu$*) is minor for both $TPPS_{2a}$ and $TPCS_{2a}$ in the organic media (Lakowicz 1999). Δf is a time-dependent parameter. This study is based on the assumption that solvent relaxation is complete prior to fluorescence emission (Lakowicz 1999; Suppan and Ghoneim 1997). In order to probe the susceptibility of $TPPS_{2a}$ or $TPCS_{2a}$ to Δf, Lippert plots (Stokes' shift versus Δf) were obtained. They were non-linear in any case ($R^2 = 0.1$–0.2). The Stokes' shift of the emission band peaked at λ_{em} ~655 nm is also not a linear function of the solvent electronic polarizability, measured as the refractive index term (Eq. 2), for neither $TPPS_{2a}$ ($R^2 = 0.831$) nor $TPCS_{2a}$ ($R^2 = 0.742$). The same observation is valid for the emission band of $TPPS_{2a}$ at ~718 nm ($R^2 = 0.809$). Deviation from linearity might be an indication of specific solvent effects (Lakowicz 1999). Nevertheless, the influences of the solvents' amphiprotic properties on the Stokes' shifts of the two compounds were also evaluated, but the results were difficult to interpret (data not shown).

Non-linear trends of the fluorescence spectral integral versus the absorbance at the excitation wavelength were observed for $TPPS_{2a}$ in 7 out of 12 solvents, i.e., tetrahydrofuran ($R^2 = 0.954$), acetonitrile ($R^2 = 0.950$), 2-propanol ($R^2 = 0.895$), methanol ($R^2 = 0.823$), chloroform ($R^2 = 0.193$), ethyl acetate ($R^2 = 0.111$), ethanol ($R^2 = 0.094$); and for $TPCS_{2a}$ in 5 out of 10 solvents, i.e., tetrahydrofuran ($R^2 = 0.978$), 2-propanol ($R^2 = 0.958$), dimethyl formamide ($R^2 = 0.922$), methanol ($R^2 = 0.873$), ethanol ($R^2 = 0.810$). The non-linear relationship between fluorescence intensity and absorbance is hard to explain, as aggregation can be ruled out. Absorbances at the excitation wavelength were kept < 0.08 (corresponding to $<10^{-7}$ M, Sec. 2.2). Reabsorption of fluorescence is, however, a possibility at least for $TPCS_{2a}$, due to its relevant absorption at ~650 nm.

2.4. Fluorescence quantum yields and solvent interactions

The fluorescence quantum yields (Φ_f) of $TPPS_{2a}$ and $TPCS_{2a}$ are influenced by properties of the solvents to a much larger extent than the spectral shifts, as presented in Table 2 and 3. Thus, the reactions taking place from the S_1* state (i.e., internal conversion, fluorescence, chemical reactions, and intersystem crossing to the excited triplet state) will highly depend on the vehicle in which the sensitizer is dissolved *in vitro* and the physiological surroundings *in vivo*. $TPCS_{2a}$ is a more efficient fluorophore than $TPPS_{2a}$ in all solvents (e.g., Φ_f ($TPCS_{2a}$)/Φ_f ($TPPS_{2a}$) = 2.2 in DMF and 6.0 in ethanol, representing the minimum and maximum relative values, respectively). Thus, the efficiency of $TPPS_{2a}$ and $TPCS_{2a}$ as photosensitizers is expected to be different when irradiated at the Soret bands. The lowest Φ_f (when comparing solvents in which both compounds are soluble) are measured in acetone (Φ_f ($TPPS_{2a}$) = 0.034; Φ_f ($TPCS_{2a}$) = 0.196). The highest Φ_f are measured in ethylene glycol (Φ_f ($TPPS_{2a}$) = 0.129; Φ_f ($TPCS_{2a}$) = 0.300) and in DMSO (Φ_f ($TPPS_{2a}$) = 0.110; Φ_f ($TPCS_{2a}$) = 0.328).

General solvent effects seem to be of some importance, as demonstrated by an increase in Φ_f as a function of the refractive index term (Eq. 2; all solvents that dissolve both compounds are included; n = 10). The relationships are however, not linear ($R^2 = 0.785$ and 0.650 for $TPCS_{2a}$ and $TPPS_{2a}$, respectively), which indicates that also specific solvent effects are important in determining the Φ_f of $TPPS_{2a}$ and $TPCS_{2a}$. Indeed, evaluation of only the Φ_f of $TPPS_{2a}$ and $TPCS_{2a}$ dissolved in the mono-alcohols (n = 4) indicates that these amphiprotic solvents are quenchers of fluorescence. There is a decrease in Φ_f as a function of increasing solvent proton donor properties (α), although the function is not linear ($TPCS_{2a}$: $R^2 = 0.846$; $TPPS_{2a}$: $R^2 = 0.612$). Fluorescence quenching might be induced by protonation of the excited state (Suppan and Ghoneim 1997). For

$TPPS_{2a}$, the effects are further emphasized by the Φ_f measured in chloroform ($\Phi_f = 0.009$) and THF ($\Phi_f = 0.062$). These solvents have equal polarity ($\pi^* = 0.58$), but chloroform is a pure proton donor ($\alpha = 0.44$; $\beta = 0$) compared to THF, which is a pure proton acceptor ($\alpha = 0$; $\beta = 0.55$). Thus, the proton donor quenches the fluorescence of $TPPS_{2a}$, possibly by introduction of additional deactivation pathways. $TPCS_{2a}$ has very low solubility in chloroform and a similar investigation was thus prevented.

Moreover, when the influence of solvent polarity is evaluated in proton accepting solvents, namely DMSO, DMF, ACN, acetone and THF, non-linear plots of Φ_f as a function of π^* or Δf are obtained.

In conclusion, the photochemical reaction pathways of the S_1^* state are likely to be influenced by interactions with the environment, i.e., physiological conditions (e.g., cell localization) *in vivo* and the vehicle *in vitro*. These effects are under further investigation by use of time-resolved fluorescence measurements.

3. Experimental

3.1. Materials

Di(monoethanolammonium) meso-tetraphenyl chlorin disulphonate ($TPCS_{2a}$) and di(triethylammonium) meso-tetraphenyl porphyrin disulphonate ($TPPS_{2a}$) were synthesized by Synthetica AS, Norway, (purity ≥98.7 %) and used as received. The compounds were stored refrigerated (+4 °C) over silica. Quinine sulphate (purity >99 %) was purchased from Fluka, Switzerland. All solvents were of p.a. grade. Ethyl acetate was dried over sodium sulphate before use.

3.2. Equipment

UV-visible absorption spectra (290–700 nm) were recorded by a Shimadzu UV-2401PC spectrophotometer. Fluorescence emission spectra were acquired on a PTI modular fluorescence system (PTI, London, Ontario, Canada). The excitation source was a 75 W xenon lamp. The monochromators were Model 101 with *f*/4 0.2-m Czerny-Turner configuration, whose entrance and exit slits were adjusted to 2 nm. Spectral correction of the emission light for the detector quantum efficiency, as well as correction for the excitation lamp spectral response, were automatically performed by the acquisition software (FeliX32 for Windows).

3.3. Methods

3.3.1. UV-Visible absorption properties

UV-visible absorption spectra were recorded of $TPCS_{2a}$ or $TPPS_{2a}$ in a series of organic solvents (n = 14) in order to evaluate the influence of solvent interactions on the absorption properties at ambient temperature. The accuracy in wavelength determination of the instrumentation was ± 1 nm. The samples were wrapped in aluminium foil prior to measurements. The concentrations were kept below 10^{-7} M.

3.3.2. Fluorescence properties

Corrected fluorescence emission spectra (n = 3) of $TPCS_{2a}$ and $TPPS_{2a}$ in a series of organic solvents were recorded at 25 ± 0.01 °C. Solutions were prepared to give an absorbance of < 0.08 at the excitation wavelength (the Soret band peak). Fluorescence quantum yields (Φ_f) were obtained by using quinine sulphate dissolved in 0.05 M H_2SO_4 as reference ($\Phi_f = 0.51$; Velapoldi and Tønnesen 2004). The calculated quantum yields were corrected for differences in sample absorbance and in refractive index of the solvents. Stokes' shifts were calculated according to Suppan and Ghoneim (1997).

3.3.3. Calculations of atomic distances in the molecular centres

The intramolecular distances (Å) between nitrogen moieties in the cores of $TPPS_{2a}$ and $TPCS_{2a}$ were calculated by means of ChemBioDraw Ultra 11.0, CambridgeSoft. The spatial atom coordinates were given by the cartesian table of x-, y- and z-coordinates of the given molecule.

Acknowledgements: This work was supported by the Norwegian Research Council. The authors are grateful to Øyvind Jacobsen, School of Pharmacy, University of Oslo, for assistance with calculations of the distances between nitrogen moieties of the molecular centres. Thanks to John Reierstad and colleagues for assistance with graphic design.

References

Akins DL, Ozcelik S, Zhu HR, Guo C (1996) Fluorescence decay kinetics and structure of aggregated tetrakis(*p*-sulfonatophenyl)porphyrin. J Phys Chem 100: 14390–14396.

Berg K, Selbo PK, Prasmickaite L, Tjelle TE, Sandvig K, Moan J, Gaudernack G, Fodstad Ø, Kjølsrud S, Anholt H, Rodal GH, Rodal SK, Høgset A (1999) Photochemical internalization: a novel technology for delivery of macromolecules into cytosol. Cancer Res 59: 1180–1183.

Berg K, Høgset A, Prasmickaite L, Weyergang A, Bonsted A, Dietze A, Lou PJ, Bown S, Norum OJ, Møllergård HMT, Selbo PK (2006) Photochemical internalization (PCI): a novel technology for activation of endocytosed therapeutic agents. Med Laser Appl 21: 239–250.

Bonnett R (1978) Nomenclature. In: Dolphin D (ed.) The Porphyrins, Vol. I Structure and Synthesis Part A, New York, pp. 12–13.

Buchler JW (1978) Synthesis and Properties of Metalloporphyrins. In: Dolphin D (ed.) The Porphyrins, Vol. I Structure and Synthesis Part A, New York, pp. 414, 453–458.

Burgoyne E (1979) Reactions of Aromatic Hydrocarbons. In: Jackson DC, Barnes S and Golden S (ed.) A short course in organic chemistry, McGraw-Hill Book Co, Singapore, pp. 139–142.

Calvert JG, Pitts Jr. JN (1966) Photochemistry, John Wiley and Sons, New York, pp. 248–258.

Cunderlikova B, Bjørklund EG, Pettersen EO, Moan J (2001) pH-Dependent spectral properties of HpIX, $TPPS_{2a}$, *m*THPP and *m*THPC. Photochem Photobiol 74: 246–252.

Dairou J, Vever-Bizet C, Brault D (2002) Self-association of disulfonated deuteroporphyrin and its esters in aqueous solution and photosensitized production of singlet oxygen by the simers. Photochem Photobiol 75: 229–236.

Dawson JB, Barker DJ, Ellis DJ, Grassam E, Cotterill JA, Fisher GW, Feather JW (1980) A theoretical and experimental study of light absorption and scattering by *in vivo* skin. Phys Med Biol 25: 695–709.

Gerhardt SA, Lewis JW, Zhang JZ, Bonnett R, McManus KA (2003) Photophysical behaviour of an *opp*-dibenzoporphyrin (2,12-diethyl-3,13-dimethyldibenzo[*g, q*]porphyrin) in micelles and organic solvents. Photochem Photobiol Sci 2: 934–938.

Ghosh A (1996) A comparison of *ortho*, *meta*, and *para* substituent effects in tetraphenylporphyrins: insights into the nature of the porphyrin-phenyl electronic interaction. J Mol Struct 388: 359–363.

Gouterman M (1961) Spectra of porphyrins. J Mol Spectrosc 6: 138–163.

Gouterman M, Wagniere GH, Snyder LC (1963) Spectra of porphyrins, part II. Four orbital model. J Mol Spectrosc 11: 108–127.

Høgset A, Prasmickaite L, Selbo PK, Hellum M, Engesæter BØ, Bonsted A, Berg K (2004) Photochemical internalization in drug and gene delivery. Adv Drug Delivery Rev 56: 95–115.

James BR (1978) Interaction of Dioxygen with Metalloporphyrins. In: Dolphin D (ed.) The Porphyrins, Vol. V Physical Chemistry Part C, New York, p. 207.

Kamlet MJ, Abboud JM, Abraham MH, Taft RW (1983) Linear solvation energy relationships. 23. A comprehensive collection of the solvatochromic parameters, π^*, α, and β, and some methods for simplifying the generalized solvatochromic equation. J Org Chem 48: 2877–2887.

Lakowicz JR (1999) Solvent Effects on Emission Spectra. In: Principles of Fluorescence Spectroscopy, 2nd ed., New York, pp. 185–207.

LeRosen AL, Reid CE (1952) An investigation of certain solvent effect in absorption spectra. J Chem Phys 20: 233–236.

Maiti NC, Mazumdar S, Periasamy N (1998) J- and H-Aggregates of porphyrin-surfactant complexes: time-resolved fluorescence and other spectroscopic studies. J Phys Chem B 102: 1528–1538.

Norum OJ, Selbo PK, Weyergang A, Giercksky KE, Berg K (2009) Photochemical internalization (PCI) in cancer therapy: From bench towards bedside medicine. J Photochem Photobiol B: Biol 96: 83–92.

Pasternack RF, Huber PR, Boyd P, Engasser G, Francesconi L, Gibbs E, Fasella P, Venturo GC, Hinds L (1972) On the aggregation of meso-substituted water-soluble porphyrins. J Am Chem Soc 94: 4511–4517.

Prasmickaite L, Høgset A, Berg K (2001) Evaluation of different photosensitizers for use in photochemical gene transfection. Photochem Photobiol 73: 388–395.

Reddi E, Jori G (1988) Steady-state and time-resolved spectroscopic studies of photodynamic sensitizers: porphyrins and phthalocyanines. Rev Chem Intermed 10: 241–268.

Seliskar CJ, Brand L (1971) Electronic spectra of 2-aminonaphthalene-6-sulfonate and related molecules. I. General properties and excited-state reactions. J Am Chem Soc: 5405–5414.

Smith GJ (1985) The effects of aggregation on the fluorescence and the triplet state yield of hematoporphyrin. Photochem Photobiol 41: 123–126.

Suppan P, Ghoneim N (1997) In: Solvatochromism. The Royal Society of Chemistry, London, pp. 1–20, 46–52, 68–80, 266–267.

Suslick KS, Watson RA (1992) The photochemistry of chromium, manganese and iron porphyrin complexes. New J Chem 16: 633–642.

Takeda J, Sato M (1995) Unusual solvent effect on absorption spectra of non-planar dodecaphenylporhyrin caused by hydrogen-bonding interactions. Chem Lett: 971–972.

Valeur B (2002) Absorption of UV-visible light. In: Molecular Fluorescence, Weinheim, p. 27.

Velapoldi RA, Tønnesen HH (2004) Corrected emission spectra and quantum yields for a series of fluorescent compounds in the visible spectral region. J Fluoresc 14: 465–472.

Winters MU, Karnbratt J, Eng M, Wilson CJ, Anderson HJ, Albinsson B (2007) Photophysics of a butadiyne-linked porphyrin dimer: influence of conformational flexibility in the ground and first singlet excited state. J Phys Chem C 111: 7192–7199.